Revista GEOCIÊNCIAS

unesp

ISSN: 1980-900X (online)

GEOCHEMISTRY AND U-Pb GEOCHRONOLOGY OF THE NEOARCHEAN GNEISSES AND PALEOPROTEROZOIC GRANITES FROM JANUÁRIA HIGH: RECORDS OF JUVENILE AND YOUTHFUL EARTH IN THE SÃO FRANCISCO CRATON NUCLEUS (BRAZIL)

GEOQUÍMICA E GEOCRONOLOGIA U-Pb DOS GNAISSES NEOARQUEANOS E GRANITOS PALEOPROTEROZÓICOS DO ALTO DE JANUÁRIA: REGISTROS DA TERRA JUVENIL E JOVEM NO NÚCLEO DO CRÁTON SÃO FRANCISCO (BRASIL)

Alexandre de Oliveira CHAVES[1], Christopher Rocha de REZENDE[1], Marco Antônio Leandro da SILVA[2], Ana Clara da Cruz PIRES[1]

[1]Universidade Federal de Minas Gerais. Instituto de Geociências. Centro de Pesquisas Manoel Teixeira da Costa. Avenida Presidente Antônio Carlos, 6627 - Pampulha, Belo Horizonte – MG.
E-mails: alochaves@yahoo.com.br; crdrezende@yahoo.com.br; anaclara2442@gmail.com
[2]Applied Isotope Research Group. Universidade Federal de Ouro Preto. Campus Morro do Cruzeiro – Ouro Preto - MG.
E-mail: marcomineral@gmail.com

RESUMO - Dentro da proposta da evolução secular do sistema Terra dividido em sete fases: "Proto-Terra" (4,57–4,45 Ga); "Terra Primordial" (4,45–3,80 Ga); "Terra Primitiva" (3,8–3,2 Ga); "Terra Juvenil" (3,2–2,5 Ga); "Terra Jovem" (2,5–1,8 Ga); "Terra Média" (1,8–0,8 Ga); e "Terra Contemporânea" (desde 0,8 Ga), os ortognaisses meta- a peraluminosos de alto-K de 2,61-2,64 Ga do Alto Januária estão inseridos no contexto de comportamento quase rígido da litosfera, no final da "Terra Juvenil". Com origem de seu protólito sugestiva de fusão parcial intracrustal dos TTG (tonalito-trondhjemito-granodiorito) locais mais antigos, esses ortognaisses são os representantes no interior do cráton do São Francisco das rochas potássicas de 2,8 Ga a 2,6 Ga encontradas em crátons arqueanos em todo o mundo, e a ocorrência dessas rochas é uma característica definidora da "Terra Juvenil". Apoiados nas evidências da atividade da tectônica de placas no Paleoproterozoico, os biotita granitos de 2,14-2,19 Ga do Alto de Januária estão inseridos no contexto da "Terra Jovem", são o registro da orogenia acrescionária delineada pela edificação de arco magmático continental nessa época e tratam-se de rochas cálcio-alcalinas do tipo I, típicas de arcos, provavelmente derivadas de uma fonte máfica de alto K associada a tonalitos.
Palavras-chave: Alto de Januária. Granitos e gnaisses. Cráton São Francisco. Terra Juvenil e Jovem. Arqueano e Paleoproterozoico.

ABSTRACT - Within the proposal of secular evolution of the Earth system divided into seven phases: "*Proto-Earth*" (4.57–4.45 Ga); "*Primordial Earth*" (4.45–3.80 Ga); "*Primitive Earth*" (3.8–3.2 Ga); "*Juvenile Earth*" (3.2–2.5 Ga); "*Youthful Earth*" (2.5–1.8 Ga); "*Middle Earth*" (1.8–0.8 Ga); and "*Contemporary Earth*" (since 0.8 Ga), the 2.61-2.64 Ga High-K, meta- to peraluminous Januária High orthogneisses are inserted in the context of almost rigid behavior of the lithosphere, by the end of the *Juvenile Earth*. With protolith origin suggestive of intracrustal partial melting of local older TTG (tonalite-trondhjemite-granodiorite), these orthogneisses are the representatives in the São Francisco craton nucleus of the 2.8 Ga to 2.6 Ga potassic rocks found in Archean cratons worldwide, and the occurrence of these rocks is a defining characteristic of the *Juvenile Earth*. Supported on evidence of the plate tectonic activity in Paleoproterozoic, the 2.14-2.19 Ga Januária High biotite granites are inserted in the context of *Youthful Earth* and they are the record of accretionary orogeny delineated by the edification of magmatic arc at that time. They are calc-alkaline, I-type rocks typical of subduction-related continental magmatic arcs. These biotite granites are probably derived from a high-K mafic source associated with tonalites.
Keywords: Januária High. Granites and gneisses. São Francisco craton. Juvenile and Youthful Earth. Archean and Paleoproterozoic.

INTRODUCTION

The crystalline basement rocks of the São Francisco Craton (SFC), outcropping on the left bank of the São Francisco River, form part of the Januária High (Alkmim & Martins Neto, 2001). The first study on geodynamic positioning, evolution and relationship between the different lithotypes that make up the Januária High, fundamental to understanding the evolution of the central portion of the SFC basement, is recent. It presents the possibility of the existence of a

Paleoproterozoic magmatic arc in the Januária High based on petrography, lithochemistry and monazite U-Th-Pb chemical ages (Rezende et al., 2018).

According to Cordani et al. (2000), the SFC corresponds to a fragment of the Gondwana supercontinent and represents the westernmost sector of the San Francisco-Congo paleocontinent (Figure 1B). This fragment is the result of the amalgamation of continental blocks (Figure 1A) in multiple and successive collisions, which began in the Archean and ended at the Rhyacian-Orosirian Orogeny (ca. 2360-2040 Ma) (Silva et al. 2016). The SFC acted as a relatively stable area during the Brasiliano orogenic cycle that occurred between 650-490 Ma. Therefore, it is delimited and bordered by mobile belts of Neoproterozoic age: to the north by the Rio Preto, Riacho do Pontal and Sergipano belts, to the south by the Ribeira belt, to the east by the Araçuaí belt and to the west by the Brasília belt (Cordani et al., 2000).

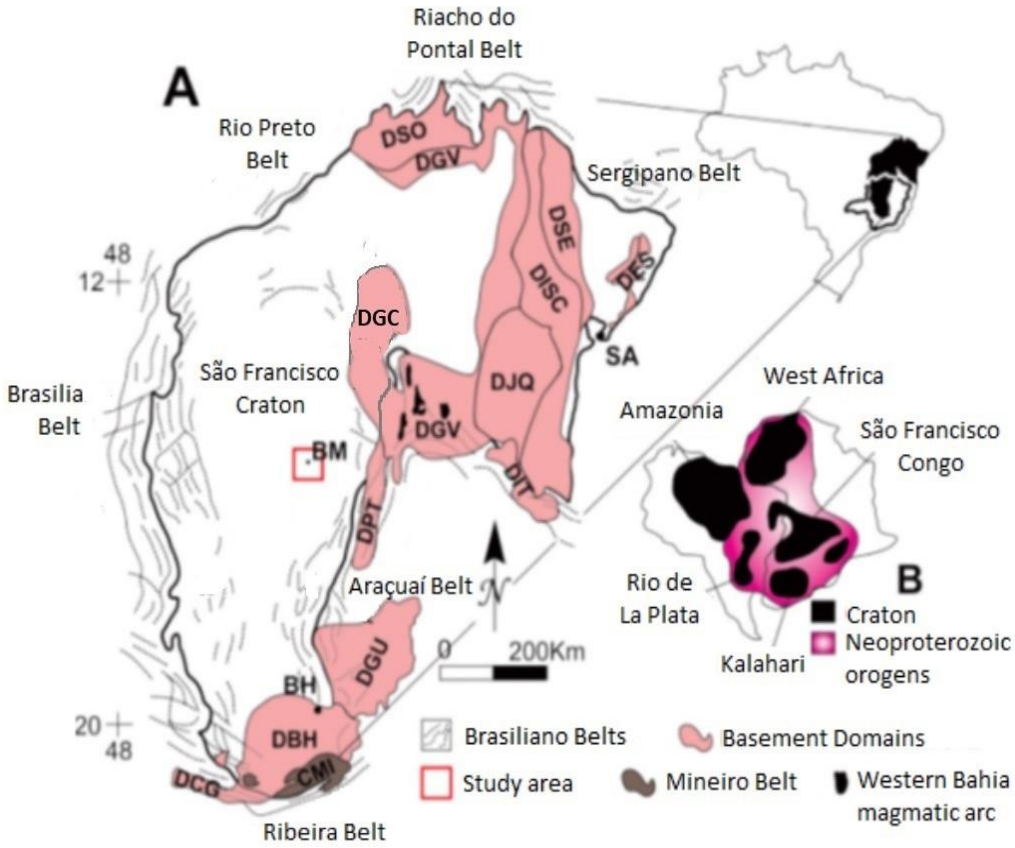

Figure 1 - (A) The São Francisco Craton, its Brasiliano marginal belts and the location of the study area. Domains from Archean to Orosirian: DBH - Belo Horizonte Domain; DCG - Campos Gerais Domain; DES - Esplanada Domain; DGU - Guanhães Domain; DGV - Gavião Domain; DGC – Guanambi-Correntina Domain; DISC - Itabuna-Salvador-Curaçá Domain; DIT - Itapetinga Domain; DJQ - Jequié Domain; DPT - Porteirinha Domain; DSE - Serrinha Domain; DSO – Sobradinho Domain; CMI – Mineiro Belt. Cities: BH = Belo Horizonte; BM = Bonito de Minas; SA = Salvador. (B) Larger cratons of South America and Africa and their relationship to the surrounding Brasiliano/Pan-African orogenic zones, in a schematic reconstruction of western Gondwana (modified from Alkmim et al., 1993; Alkmim & Martins-Neto 2001; Silva et al., 2016; Barbosa et al., 2020).

Within the context of the SFC basement shown in figure 1A, the Belo Horizonte Domain (DBH) in the southern region of the craton, is constituted predominantly by banded and migmatized TTG (tonalite-trondhjemite-granodiorite) gneisses formed in the Archean between 3.0 and 2.6 Ga. (Machado et al., 1989; Alkmim & Marshak, 1998). During the Paleoproterozoic, the evolution of the basement has its initial milestone related to the opening of the Minas Basin during the Siderian (ca. 2.4 Ga – Babinski et al., 1995; Teixeira et al., 2015), which subsequently gave rise to a tectonic inversion and reworking of the DBH gneisses through a long-term orogenic system represented by the Mineiro Belt (CMI - Teixeira et al., 2000, 2015; Barbosa et al., 2015).

At the CMI, the period of greatest plutonism described occurred between 2.2-2.1 Ga with some examples of juvenile crustal growth at 2350 Ma, represented by the Lagoa Dourada suite and the Resende Costa granite (Noce et al., 2000; Silva et al., 2002; Noce et al., 2007; Campos &

Carneiro, 2008; Ávila et al., 2010; Seixas & Stevenson, 2012; Silva et al., 2012).

Concerning the Gavião Domain (DGV), Cruz et al. (2016) characterize the Western Bahia magmatic arc as a long-duration arc system during the Rhyacian-Orosirian developed contemporaneously with the CMI. U-Pb data from Barbosa et al. (2020) place the evolution Guanambi-Correntina block (DGC) contemporaneous with the Gavião block, but it was formed as an independent unit in central north SFC. In the Porteirinha Domain (DPT), Silva et al. (2016) characterize a segment of the Rhyacian-Orosirian belt dated at 2150 Ma and TTG rocks with 3.37 Ga (Fig. 1A).

From the Statherian onwards, regional taphrogenetic events related to the opening of the Espinhaço rift affected the SFC. Pedrosa-Soares & Alkmim (2011) describe the events as: E1 (Statherian, 1.77-1.7 Ga), E2 (Calymmian, 1.57 - 1.5 Ga), E3 (Stenian, 1.18 - ? Ga), E4 (at the Stenian-Tonian boundary, ca. 1 Ga), E5 (Tonian, 930 - 850 Ma) and E6 (Cryogenian, 750-670 Ma). The E1 event (also known as Statherian Taphrogenesis) has as its most important records the development of the rift and the deposition of sedimentary and volcanic units at the base of the Espinhaço Supergroup. The last regional tectonic event corresponds to the Brasiliano orogenic event (650-490 Ma), which Pedrosa-Soares et al. (2001) describe as responsible for the reworking of large segments of the SFC basement, represented mainly by the Guanhães (DGU) and Porteirinha (DPT) domains within the Araçuaí belt.

In this study, the focus was on producing data on basement formation processes in the central portion of the craton and relating them to the processes described for other basement exposures on a cratonic scale, linking these processes to the *Juvenile and Youthful Earth phase*s described in Cawood et al. (2022). These data came from the characterization of the granitic and gneissic rocks belonging to the Januária High, based on field information, petrology, lithochemistry and unprecedented U-Pb isotopic ages in zircon. These informations constraints the existence of a Paleoproterozoic orogenic cycle, which would include the evolution of a magmatic arc in the Januária High region.

GEOLOGICAL SETTING

The Januária High corresponds to an elevation of the crystalline basement, which reaches altitudes close to 600 meters on the surroundings of the Bonito de Minas city (Figure 2A). This elevation, according to Iglesias (2007), was probably generated by the action of normal Neoproterozoic faults, or older ones, reactivated during the sedimentation of the Bambuí Group. These faults would form a horst and graben system in an EW and N40-50W direction (Costa, 1978; Beurlen, 1973) with embedded mafic dykes (Paulsen et al., 1974). Figure 2B shows the distribution of the main units in the Januária High region and Table 1 a brief description of them.

The SFC gneissic and granite rocks outcropping on the left bank of the São Francisco River are described by CODEMIG's mapping projects as part of the Januária High. These occur in windows that expose the basement of the SFC along the drainages of the main rivers and streams in the municipalities of Januária, Bonito de Minas and Cônego Marinho and make up a set of deformed and undeformed rocks (Almeida & Uchigasaki, 2003). In the region of Bonito de Minas (MG), the basement of the SFC is composed of gneisses and granitoids, which constitute the only window to the core of the SFC with ages older than 1.8 Ga. These rocks are overlaid by Precambrian (Bambuí Group) and Phanerozoic (Santa Fé, Areado and Urucuia Groups) coverings that constitute the São Francisco Basin (Figure 2). The Precambrian units of the São Francisco Basin were partially deformed during the Neoproterozoic by the Brasiliano Orogeny.

The rocks that make up the Januária High appear mainly in the form of in situ blocks or exposures with a higher concentration in drainages (Figure 3A).

Their contacts were not observed by the limited number of exposures. The geophysical maps used (Figures 3B and 3C) correspond to areas 5 and 18 produced by the Aerogeophysical Survey of the State of Minas Gerais, carried out by CODEMIG (2008/2009 and 2010/2011), with a flight height of 100 meters and spacing of 500 meters. The positioning of the amplitudes resulting from the analytical signal (Figure 3B) reveals lineaments of high magnetic intensity related to mafic dykes (diabases) of NW-SE direction referring to the 1.76 Ga Januária swarm (Chaves & Correia Neves, 2005; Chaves &

Rezende, 2019; Chaves et al. 2021). The association of the Th-U-K ternary gamma-spectrometric map with the shaded relief (Figure 3C) allows defining areas of high potassium mainly associated with drainages. The high K pattern is due to the presence of outcropping gneisses and granitoids especially in the central area.

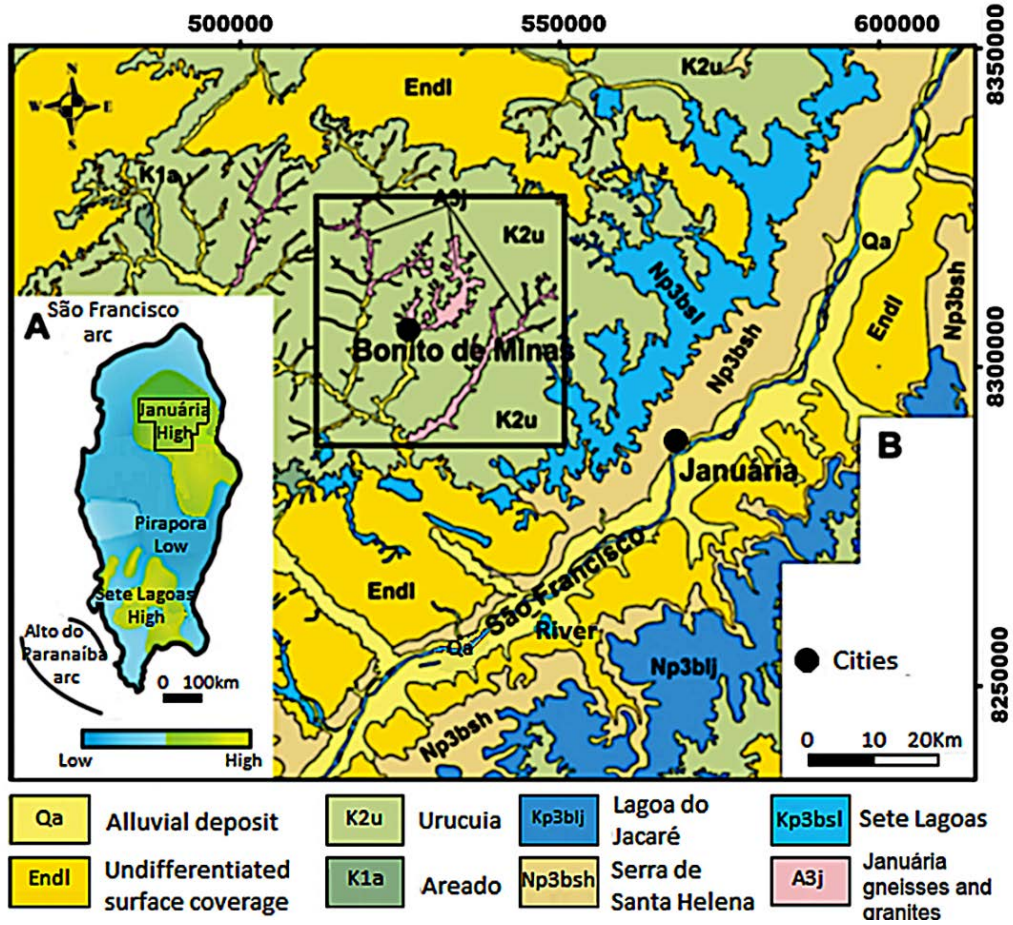

Figure 2 - (A) Gravimetric features of the SFC basement with emphasis on Januária High. **(B)** Geological map of the Januária High region with the delimitation of the study area (Modified from Alkmim & Martins-Neto, 2001; CODEMIG, 2014).

The rocks that make up the basement of the SFC in the region of Bonito de Minas are grouped into gneisses (deformed) and granitoids (undeformed). Among the deformed rocks that make up the Januária High, there are gneisses and migmatitic gneisses. The gneisses present a fine to medium-grained granolepidoblastic texture (Figures 4A and 4B). Local banding of these rocks is marked by the alternation of centimetric bands (approximately 3 cm) rich in feldspar and quartz, and thin bands rich in biotite and amphibole.

The migmatitic gneiss presents coarse granulation, foliation marked by the biotite orientation and phlebitic and stictolitic texture (figure 4C and 4D), representing a metatexite with texture of spots according to the classification of Sawyer (2008). In this rock, the leucosome occurs as misshapen portions of granulation slightly coarser than the melanosome. Inside the leucosome, dark spots are also observed, which represent the concentration of mafic minerals, indicating partial melting in situ in the initial stages.

The granitoids that make up the crystalline basement of the region correspond to granites and granodiorites of different textures (Figure 5). Fine to medium-grained, dark gray to beige granites represent the greatest exposure of these rocks and include intrusive bodies with rare igneous banding (Figures 5A, 5B, 5C). Associated with these bodies is a pink granite, which is inequigranular, phaneritic with very coarse grains and injected by late lamprophyric small bodies (Figure 5D). In its mineralogy, subhedral pink K-feldspar crystals, yellowish plagioclase and quartz stand out, with anhedral amphibole and biotite occurring as dark masses. There is also a porphyritic granite, which is massive, light gray and beige with beige euhedral K-feldspar phenocrysts measuring up to 3 cm (Figures 5E and 5F). Composing its matrix, crystals of subhedral feldspar and anhedral quartz occur.

Table 1 - Stratigraphic column with the main units, ages and lithologies of the Januária High region in the study area. Sources: 1 CODEMIG (2014); 2a Geobank (2015a); 2b Geobank (2015b); 2c Geobank (2015c); 3 Dias-Brito et al. (1999); 4 Babinski & Kaufman (2003); 5 Nobre-Lopes (2002); 6 Babinski (1993); 7 Radambrasil (1982); 8 Costa & Branco (1961); 9 Pflug & Renger (1973).

Code	Supergroup	Group	Formation	Lithology	Age
Qa	Alluvial deposit			Unconsolidated clastic sediments	Quaternary[1]
Endi	Undifferentiated surface cooverage			Clastic and ferruginous lateritic sediments	Neogene[1]
K2u		Urucuia		sandstones, quartz, reddish and white, of fine to medium sand granulometry, with rounded, well-selected grains and scarce clay matrix[8]. Conglomeratic sandstone, sandstone, shale or claystone, conglomerate[1].	Upper Cretaceous[2c] (99,6 Ma – 65,6 Ma)
K1a		Areado		shale, feldspathic sandstone, lithic sandstone, conglomeratic sandstone, polymitic conglomerate, siltstone[1].	Barremian – Aptian[3]
NP3blj	São Francisco[9]	Bambuí	Lagoa do Jacaré	Oolitic and psolitic limestones, dark gray, fetid, crystalline with interspersed siltstones and marls[1].	Ediacaran[2a] (542,1 Ma – 630 Ma)
NP3bsh			Serra de Santa Helena	Siltstones, claystones, slates and greenish shales limestone lenses[8].	Ediacaran[2b] (542,1 Ma – 630 Ma)
NP3bsl			Sete Lagoas	Limestone and dolomite occasionally with marls and pelitic lenses[8].	740 +/- 22 Ma (Pb/Pb)[4] 600 Ma (87Sr/88Sr)[5] 686 +/-69 Ma (Pb/Pb)[6]
A3j	Januária High			TTG-type banded gneisses and associated granitoids[1].	1.970 Ma (Rb/Sr)[7]

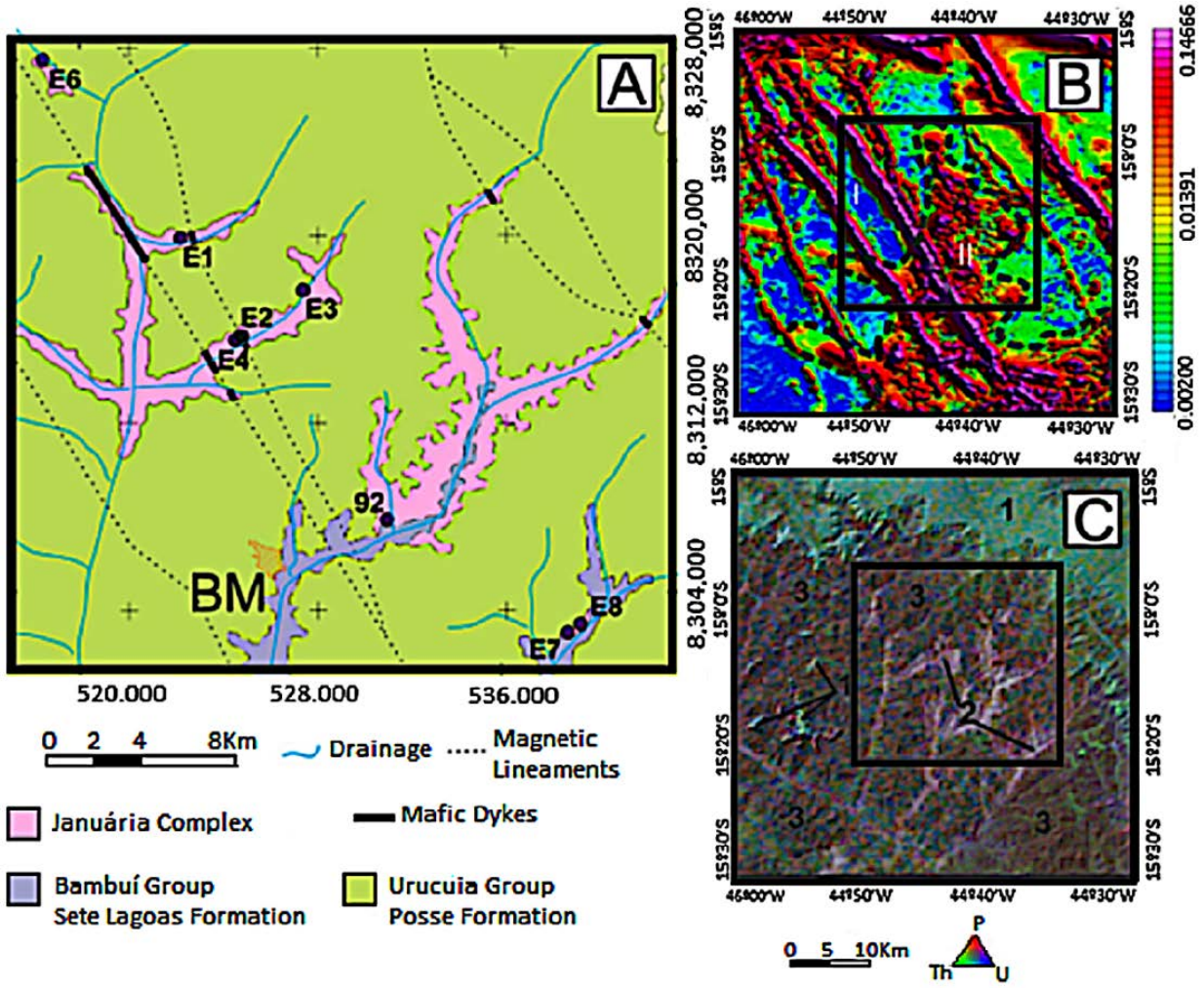

Figure 3 - (A) Location map of granitic and gneissic rocks sampled in windows that expose the SFC basement along local drainages. BM = Bonito de Minas (Modified from Uhlein *et al*., 2015). **(B)** Magnetometric map (analytical signal) of the Catolé sheet divided into anomaly domains: I = low analytical signal and II = high analytical signal (Modified from CODEMIG, 2014). **(C)** Ternary map of potassium, uranium and thorium channels in RGB pattern associated with shaded relief. Gamma spectrometric domains indicated in the figure and explained in the text (Modified from CODEMIG, 2014).

METHODS

During the field work, 14 samples of the rocks that make up the basement around Bonito de Minas were collected. In the laboratories of the Manoel Teixeira da Costa Research Center (IGC/UFMG), 15 thin sections of the samples were made, which were used in the micropetrographic studies in an optical microscope of polarized light. Subsequently, 9 samples were selected and pulverized in a tungsten mill and sent to the SGS-Geosol Laboratory. There, the major elements and five trace elements (Ba, Nb, Sr, Y, Zr) were analyzed by Inductively Coupled Plasma Optical Emission Spectrometry (ICP-OES) and seven other trace elements (Rb, Ta, Sn, Hf, Ni, Th, U) together with 14 rare earths elements were analyzed by Inductively coupled plasma mass spectrometry (ICPMS).

Loss on fire was due to weight difference after heating at 1000 °C. In the data processing, ArcMap 10.2 and TrackMaker Pro softwares were used for field and geophysical data and GCDkit 4.0 for geochemical and petrographic data.

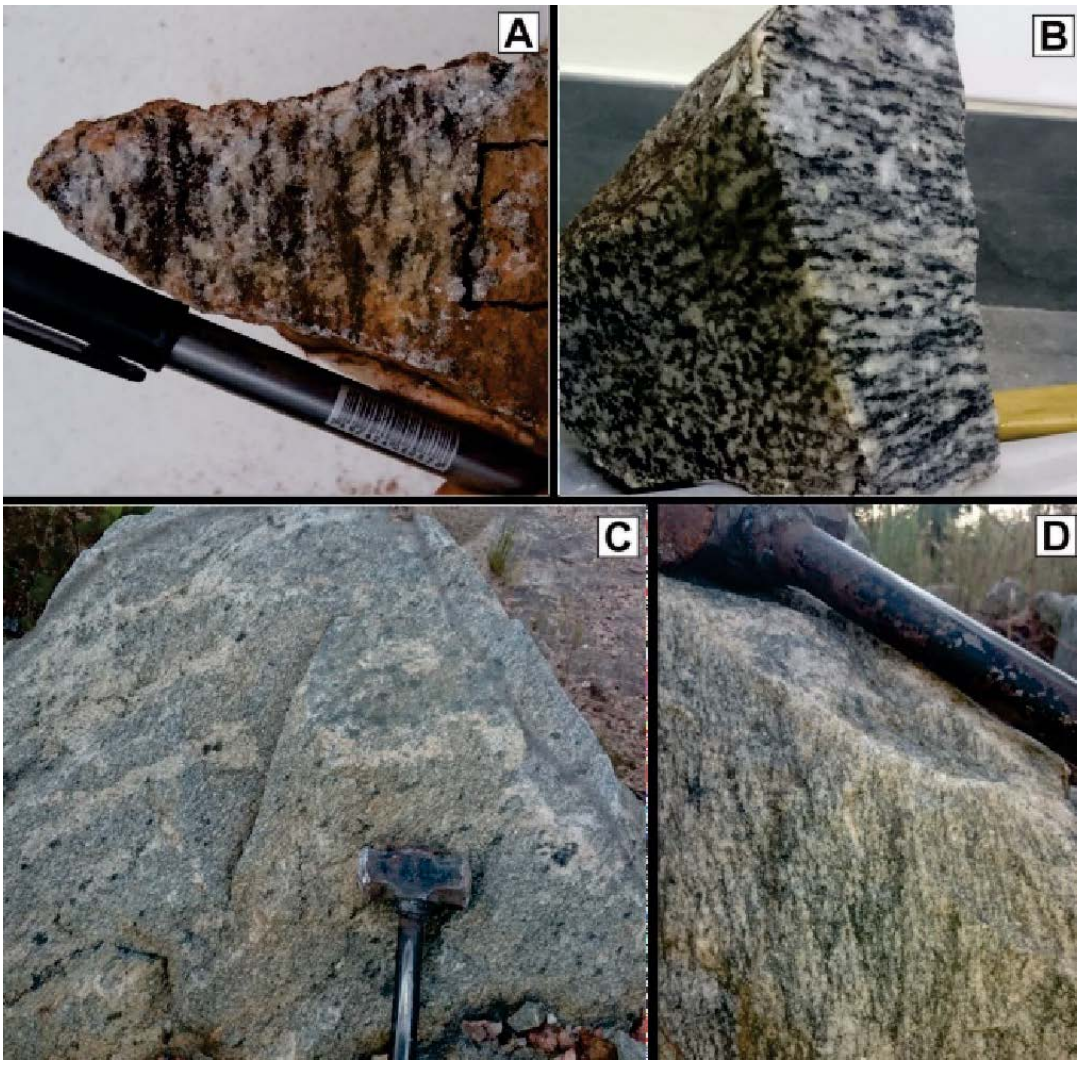

Figure 4 - Different features of the gneisses that make up the Januária High. **(A)** Coarse-grained gneiss with fine banding marked by thin layers of biotite (Sample E3). **(B)** Detail of banding in the gneiss (Sample E7). **(C)** Migmatitic gneiss with phlebitic and stictolitic texture (Sample E8). **(D)** Detail of foliation in migmatitic gneiss (Sample E8).

Geochronological U-Pb zircon data were acquired using the laser ablation sector field inductively coupled plasma mass spectrometry (LA-SF-ICP-MS) in the Isotopic Geochemistry Laboratory in the Federal University of Ouro Preto (UFOP). Samples were crushed and undergo through a disk mill. The obtained material was then concentrated using a pan, dried between 50 and 70 ºC and the magnetic fraction was separated using a neodymium magnet. The nonmagnetic fraction of the concentrated material was separated into a portion with density superior than 3.31 and other with density inferior than 3.31 using a decantation funnel and diiodomethane. The denser material undergone Frantz magnetic separator machine for the segregation in diamagnetic and

paramagnetic portions. Diamagnetic material was mounted in acrylic resin and polished using alumina powder. Optical zircon images were obtained in a binocular loupe.

U-Pb analysis were obtained using an Element 2 Thermo Finnigan coupled with a Photon-Machines 193nm laser system. Data were acquired using peak jumping mode with background measurement during 20 seconds, zircon ablation during 20 seconds and 30 micrometers spot size. Data reduction was done in GLITTER Software. Common lead correction was applied using a Ms Excel spreadsheet program (Gerdes & Zeh 2006) based on Stacey & Kramers (1975) Pb composition model. GJ-1, BB and Plesovic age reference patterns, with ages from 600 to 300 Ma, have been used for control. Isoplot (Ludwig, 2001) was used and the errors were presented in 2 *sigma*. The results table was built according to Horstwood et al. (2016).

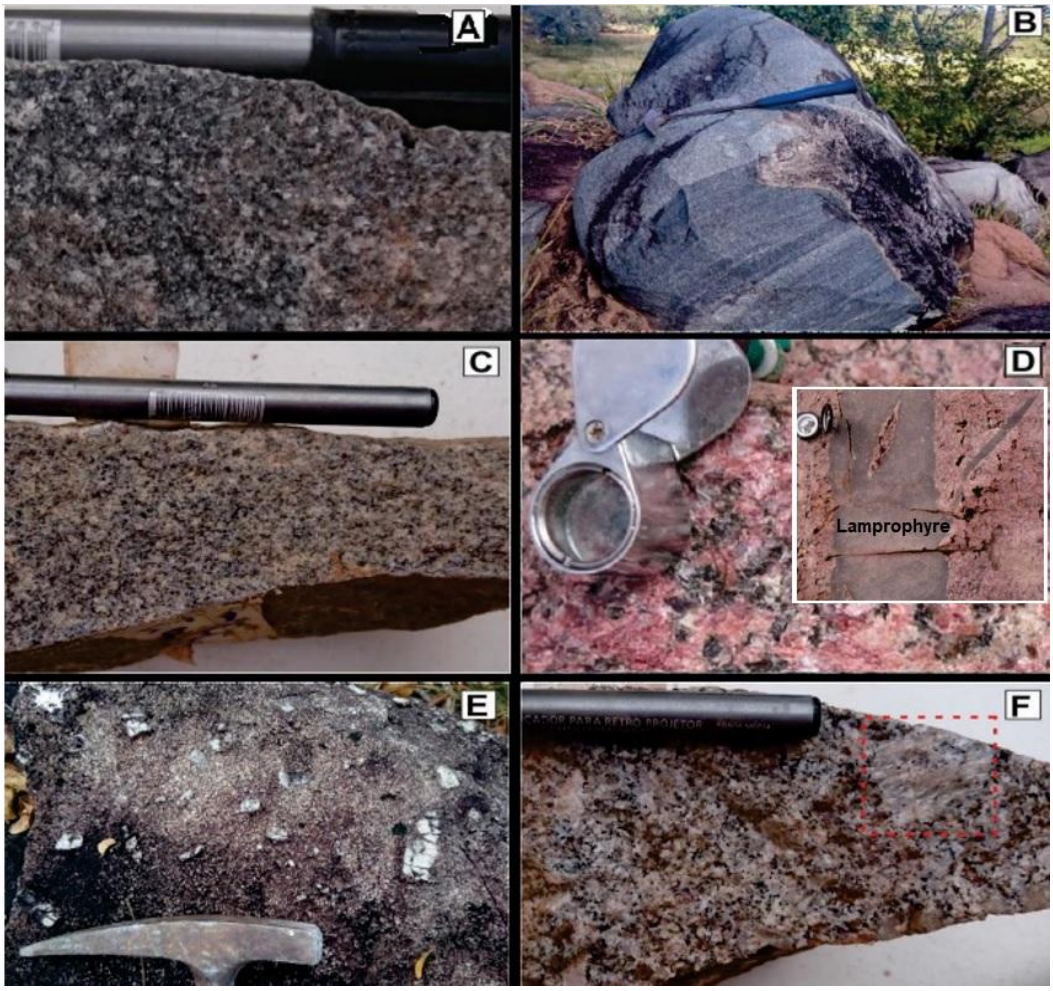

Figure 5 - Different features of the granitoids that make up the Januária High. **(A)** Dark gray, equigranular, medium-grained granite. (Sample E1B). **(B)** Typical block field outcrop showing two portions of different granulation (igneous banding) of gray equigranular granite (Site E6). **(C)** Light gray and beige granite, medium phaneritic and equigranular (Sample E2A). **(D)** Pink granite, inequigranular with very coarse granulation (Sample 92A). Late Injections of lamprophyric dark bodies are found inside pink granite **(E)** K-feldspar phenocrystals highlighted by weathering. **(F)** Detail of the porphyritic granite. Red square showing a phenocrystal (Sample E2B).

RESULTS

The micropetrographic and lithochemical results below correspond to reinterpreted data from Rezende et al. (2018). The U-Pb geochronology data in zircon are unpublished until now.

Micropetrography

The modal percentage values, for the different thin sections described, are listed in Table 2 and the classification of the samples according to Streckeisen's QAP diagram (1974) in Figure 7A.

Gneisses

The orthogneiss samples correspond to rocks with penetrating foliation, of granodioritic (site E3 in figure 3A) to granitic (site E7 and E8 in figure 3A) modal composition, and fine to medium-grained granolepidoblastic texture (Figures 6A and 6B). In the essential mineralogy, quartz shows undulating extinction and is partially recrystallized and, in this case, occurs as anhedral

Table 2 - Modal percentage of minerals present in the samples and occurrence of accessory minerals (marked with "x"). Adapted from Rezende *et al*. (2018).

modal % of minerals		Gneisses			Granite					
		E3	E7	E8	E1B	E2A	E2B	E6A	E6B	92A
Essentials	Quartz	26	38	40	32	36	30	36	32	38
	Potassium feldspar	16	36	35	19	29	29	31	33	39
	Plagioclase	43	23	20	34	30	33	28	30	16
	Biotite	10	3	5	10	5	8	5	5	4
	Amphibole	5	0	0	5	0	0	0	0	3
Accessories	Apatite	x	x	x	x	x	x	x	x	x
	Allanite	x	x	x	x	x	x	x	x	x
	Titanite									
	Zircon	x	x	x	x	x	x	x	x	x
	Muscovite		x			x			x	
	Opaque	x			x					x
	Garnet			x						
	Monazite			x						

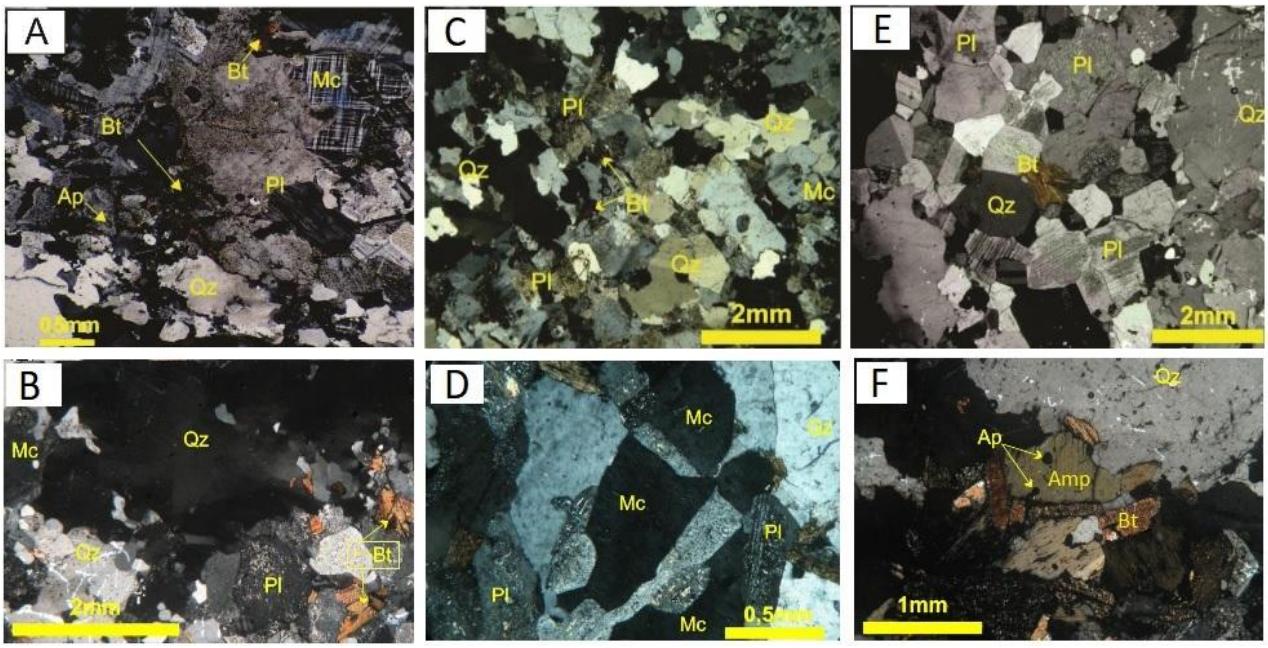

Figure 6 - Photomicrographs of the orthogneisses and biotite granites of the Januária High, obtained in a petrographic microscope under transmitted light and crossed polarizers (adapted from Rezende et al., 2018). **(A)** Migmatitic gneiss E8. **(B)** Gneiss E3. **(C and D)** Biotite granite E2A. **(E and F)** Pink biotite granite 92A. Mineral abbreviations according to Whitney & Evans (2010). Bt = biotite, Mc = microcline, Pl = plagioclase, Qz = quartz, Ap = apatite, Amp = Amphibole.

grains. The plagioclase is partially saussuritized. The potassium feldspar present is the microcline with tartan-type twinning, with myrmekite growth in contact with the quartz. There are hydrated minerals in the gneiss, represented by biotite and amphibole, the latter found only in sample E3. The amphibole present is hornblende, with strong pleochroism from green to brown and with apatite inclusions. The biotite is pleochroic from light brown to brown and arranged in an oriented manner according to the gneissic foliation. In accessory mineralogy, not only subhedral zircon is identified, forming alteration halos in biotite, but also apatite, allanite and rare opaques. Garnet and monazite were found as accessory minerals only in sample E8 and muscovite in sample E7.

Biotite Granites

This group of rocks includes samples E1B (site E1 in figure 3A), E2A, E2B (both from site E2 in figure 3A), E6A, E6B (both from site E6 in figure 3A) and the pink granite from site 92 in figure 3A.

These rocks generally have a granitic modal composition, holocrystalline texture, inequigranular, fine to medium-grained, with approximately 5% of biotite, which occurs as fine flakes with alteration edge to chlorite. Another hydrated mineral is amphibole, present in samples E1B and 92A, which occurs as elongated crystals with

weak pleochroism in shades of green. Among the thin-sections described, the E2B sample stands out for its porphyritic holocrystalline texture with microcline phenocrysts of up to 3 cm and a fine to medium-grained inequigranular matrix. Quartz has undulating extinction, the plagioclase is saussuritized and the potassium feldspar present is the perthitic microcline, with tartan-type twinning. Close to some of these contacts, it is possible to observe the presence of myrmekite. In sample E2A, the microcline is subhedral, sometimes sericitized and with inclusions of biotite and plagioclase (Figure 6C and 6D). The accessory mineralogy shows subhedral apatite, euhedral to subhedral zircon, muscovite in samples E2A and E6B, rare opaque minerals and allanite.

The only pink granite biotite is represented by sample 92A, being coarse-grained and with inequigranular phaneritic texture. Biotite is associated with amphibole, probably hornblende (Figures 6E and 6F), with pleochroism from green to brown. The plagioclase presents a subhedral shape, saussuritized, with greater intensity in the center than in the edges, indicating a normal compositional zoning. Quartz exhibits undulating extinction and the perthitic microcline has a poikilitic texture with coarse to very coarse grains, tartan-type twinning.

In the accessory mineralogy, allanite stands out, which when included in biotite forms pleochroic halos in it. There are also rare opaque minerals and euhedral to subhedral zircon.

Lithochemistry

Table 3 presents the total rock chemical data of major elements (% by weight), trace elements and rare earths (ppm) of 3 samples of gneisses and 6 samples of biotite granites. It also presents the respective CIPW normative composition data. The data (% by weight) of major elements show that the rocks have SiO_2 above 67%, Al_2O_3 values between 12 and 16%, FeO_t less than 4.5% and MgO generally below 1%. They present values of K_2O and Na_2O above 3% and great variation in CaO contents (1 to 2.7% for granites and 0.7 to 3.2% for gneisses).

In the TAS diagram (Figure 7B), all investigated rocks have granitic composition, except the E3 gneiss which is granodiorite, confirming the petrographic investigations (Figure 7A). According to the classification of igneous rocks proposed by Frost *et al*. (2001) and Peccerillo & Taylor (1976), samples of the Januária High are mostly peraluminous and High-K calc-alkaline (Figures 7C, 7D and 7E), with the exception of E3 gneiss, which is metaluminous. According to the diagrams by Whalen et al. (1987) (Figures 7F and 7G), there is a tendency for pink biotite granite (sample 92A) to position itself in the field of type-A granites while the other granites in the fields of type-I and type-S granitoids. In the diagram of Chappell & White (2001) it is noticed that the granites essentially correspond to type-I (Figure 7H).

In the diagram of rare-earth elements – REE – (Figure 7I), normalized to chondrite according to Boynton (1984), the gneisses show a discreet fractionation of light REEs in relation to the heavy ones, with a notable negative Eu anomaly. The curves of the biotite granites differ from the curves of the gneisses and generally present slight positive Eu anomalies and strong fractionation of light REEs compared to the heavy REEs from the Dy, as well as the pink granite biotite (sample 92A). The curve pattern of the High-K calc-alkaline granites of Januária is similar to the pattern of the Peruvian coastal batholith of the Andean magmatic arc of Atherton et al. (1979). The diagram of incompatible elements, normalized according to the MORB of Pearce (1983), reveals that the samples present, in general, negative anomalies of Sr, Ta, Nb, P and Ti (Figure 7J), being Ta and Nb anomalies normally indicative of subduction processes in environments of plate convergence near continental magmatic arcs. The pattern of the curves of Januária calc-alkaline granites is similar to the pattern of type I granites by Winter (2001).

In the diagrams by Pearce et al. (1984) (Figures 7K and 7L), the granites are classified as magmatic arc setting and the pink granite biotite as post-collisional. Finally, the diagram by Laurent et al. (2014) allows us to infer that the Januária biotite granites are probably derived from a mafic source of high potassium associated with tonalites (Figure 7M). The magmas of the Januária biotite granites seem to have undergone processes of magmatic differentiation by fractional crystallization, attested by the correlation trends between their samples (except sample 92A) in Harker diagrams of SiO_2 versus oxides of major elements and trace elements such as Sr, Zr, Y, La and Ce (Figure 8).

Table 3 - Chemical and normative composition of samples from the Januária High (LOI = loss on ignition, iron expressed as FeOt). Adapted from Rezende et al. (2018).

	Gneisses			Granites					
Sample	**E3**	**E8**	**E7**	**E1B**	**E2A**	**E2B**	**E6A**	**E6B**	**92A**
Major elements (%)									
SiO_2	68.58	74.23	73.91	67.96	72.01	68.24	71.83	73.8	74.43
TiO_2	0.44	0.18	0.21	0.54	0.22	0.41	0.37	0.17	0.18
Al_2O_3	15.20	13.29	14.18	15.57	14.04	15.81	15.37	15.22	12.76
FeOt	4.31	1.60	1.72	3.24	1.65	2.94	2.32	1.13	2.53
CaO	3.26	0.79	1.36	2.74	1.32	2.08	2.05	1.90	1.00
MgO	1.20	0.28	0.29	0.72	0.45	0.78	0.64	0.35	0.13
MnO	0.08	0.03	0.03	0.05	0.04	0.05	0.03	0.02	0.04
K2O	3.47	4.45	4.58	3.43	3.78	3.37	3.09	4.02	4.64
Na_2O	3.69	3.31	3.46	3.83	4.05	4.35	4.25	4.08	3.17
P_2O_5	0.06	0.02	0.01	0.14	0.04	0.11	0.07	0.05	0.02
LOI	0.63	0.55	0.80	0.78	0.78	0.89	0.87	0.66	0.30
Total	**100.93**	**98.74**	**100.57**	**99.02**	**98.38**	**99.03**	**100.92**	**101.42**	**99.21**
Normative minerals - CIPW (%)									
Q	25.48	35.9	32.95	26.01	30.61	24.74	30.14	30.24	35.96
C	0	1.64	1.08	0.91	0.98	1.49	1.47	0.82	0.75
Or	20.51	26.3	27.07	20.27	22.34	19.92	18.26	23.76	27.42
Ab	31.22	28.01	29.28	32.41	34.27	36.81	35.96	34.52	26.82
An	14.66	3.79	6.68	12.68	6.29	9.60	9.71	9.1	4.83
Hy	2.99	0.7	0.72	1.79	1.12	1.94	1.59	0.87	0.32
Il	0.17	0.06	0.06	0.11	0.09	0.11	0.06	0.04	0.09
Hm	4.31	1.60	1.72	3.24	1.65	2.94	2.32	1.13	2.53
Tn	0.79	0	0	0	0	0	0	0	0
Ru	0.03	0.15	0.18	0.48	0.18	0.35	0.34	0.15	0.14
Ap	0.14	0.05	0.02	0.33	0.10	0.26	0.17	0.12	0.05
Total	**100.3**	**98.19**	**99.76**	**98.24**	**97.61**	**98.16**	**100.03**	**100.75**	**98.91**
Trace elements (ppm)									
V	43	34	0	44	26	66	53	18	25
Co	108.7	110.6	143.1	123.6	137.6	113.3	127.5	149.4	149.9
Ni	9	11	6	11	10	13	17	9	9
Zn	44	34	16	37	32	38	43	11	62
Ga	16.7	20.4	18	20.4	19.1	19.1	19.5	17.6	19.7
Rb	90.8	245.6	167.7	87.7	114.4	95.9	108.3	93.7	64.5
Sr	212	46	217	438	263	416	293	272	195
Y	45.35	48.79	14.9	8.27	9.88	14.29	8.33	4.43	21.69
Zr	216	144	174	271	130	193	200	126	326
Nb	5.97	23.74	8.76	7.97	6.27	5.94	8.64	2.67	6.58
Ba	1071	169	1258	1806	1038	1346	1080	1277	3317
Hf	6.08	4.57	4.48	6.17	3.68	4.65	4.54	3.07	7.68
Ta	0.09	1.22	0.55	0.48	0.44	0.15	0.2	0.05	0.17
Th	8.4	33.2	11.8	13.7	10.7	10.3	9.8	12.6	9.6
U	0.71	31.31	2.44	1.41	3.27	1.42	2	3.88	1.16
Rare earth elements (ppm)									
La	33.9	38	32.5	60	30.1	43.7	43.5	29.3	101.8
Ce	72.9	71.1	66.4	102.4	51.3	76.7	62.2	53	199.2
Pr	9.03	7.83	7.43	10.42	5.46	8.29	6.25	5.44	22.45
Nd	35.8	27.1	26.3	35.2	19.4	28.7	21.3	18.3	83.9
Sm	7.6	6.8	5.3	4.8	3.6	4.8	3.3	2.8	12.2
Eu	1.12	0.31	0.82	1.48	0.89	1.08	1.01	0.9	4.07
Gd	7.95	7.34	4.48	3.41	2.95	4.01	2.68	2.02	9.15
Tb	1.28	1.34	0.63	0.4	0.38	0.56	0.34	0.23	1.11
Dy	7.67	8.25	2.95	1.55	1.74	2.69	1.48	0.81	4.88
Ho	1.62	1.63	0.56	0.32	0.35	0.53	0.31	0.17	0.92
Er	4.89	4.69	1.5	0.88	1.02	1.52	0.9	0.46	2.53
Tm	0.7	0.66	0.21	0.12	0.15	0.23	0.12	0.06	0.35
Yb	4.6	4.1	1.4	0.8	1.0	1.4	0.8	0.4	2.3
Lu	0.67	0.59	0.2	0.12	0.15	0.21	0.12	0.06	0.37

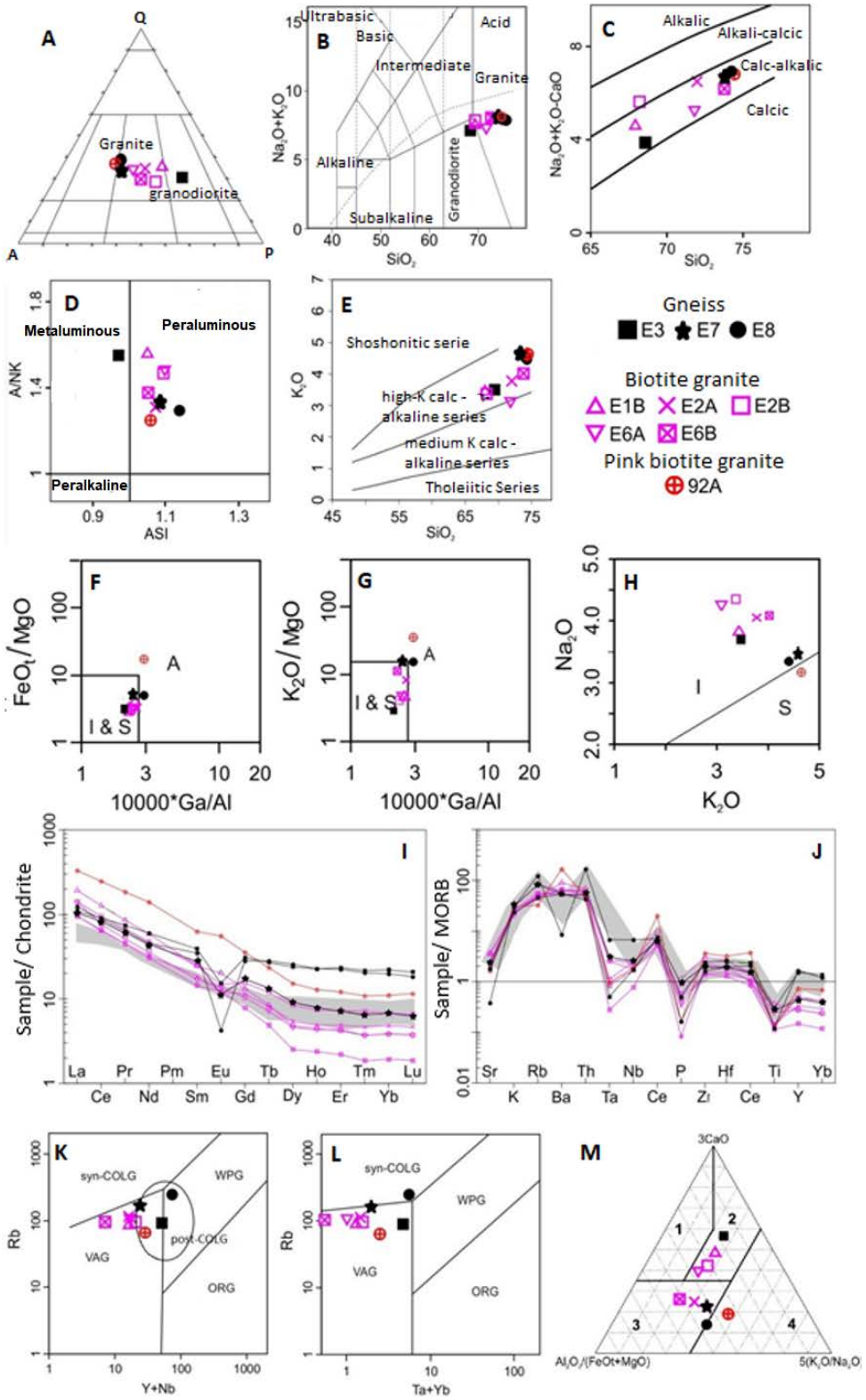

Figure 7 - Classification of the rocks of the Januária High (Adapted from Rezende et al., 2018). **(A)** QAP modal composition diagram (Streckeisen, 1974). **(B)** TAS Diagram (Le Bas et al., 1986). **(C e D)** MALI and ASI diagrams, respectively, according to Frost et al. (2001). **(E)** K_2O versus SiO_2 diagram according to Peccerillo & Taylor (1976). **(F e G)** Classification diagrams of anorogenic granites according to Whalen et al. (1987). **(H)** Diagram of division between type-I and S granites according to Chappell & White (2001). **(I)** Arachnogram of rare-earth elements normalized according to the chondrite of Boynton (1984). Reference standard, in grey, for the Peruvian coastal batholith of Atherton *et al*. (1979). **(J)** Diagram of incompatible elements normalized according to MORB of Pearce (1983). In gray, reference standard for type I granites of Winter (2001). **(K e L)** Diagrams of tectonic discrimination of granitoids according to Pearce et al. (1984) (modified by Pearce, 1996). ORG = oceanic ridge granites, WPG = intraplate granites, VAG = granites from volcanic arcs, syn-COLG = syn-collisional granites and post-COLG = post-collision granites. **(M)** ternary diagram $Al_2O_3/(FeO_t+MgO)$; 3*CaO; 5*(K_2O/Na_2O) representing the possible source of the rocks of the Januária High (Laurent et al., 2014). 1 = Low potassium mafic rocks, 2 = High potassium mafic rocks, 3 = Tonalites e 4 = Metasediments.

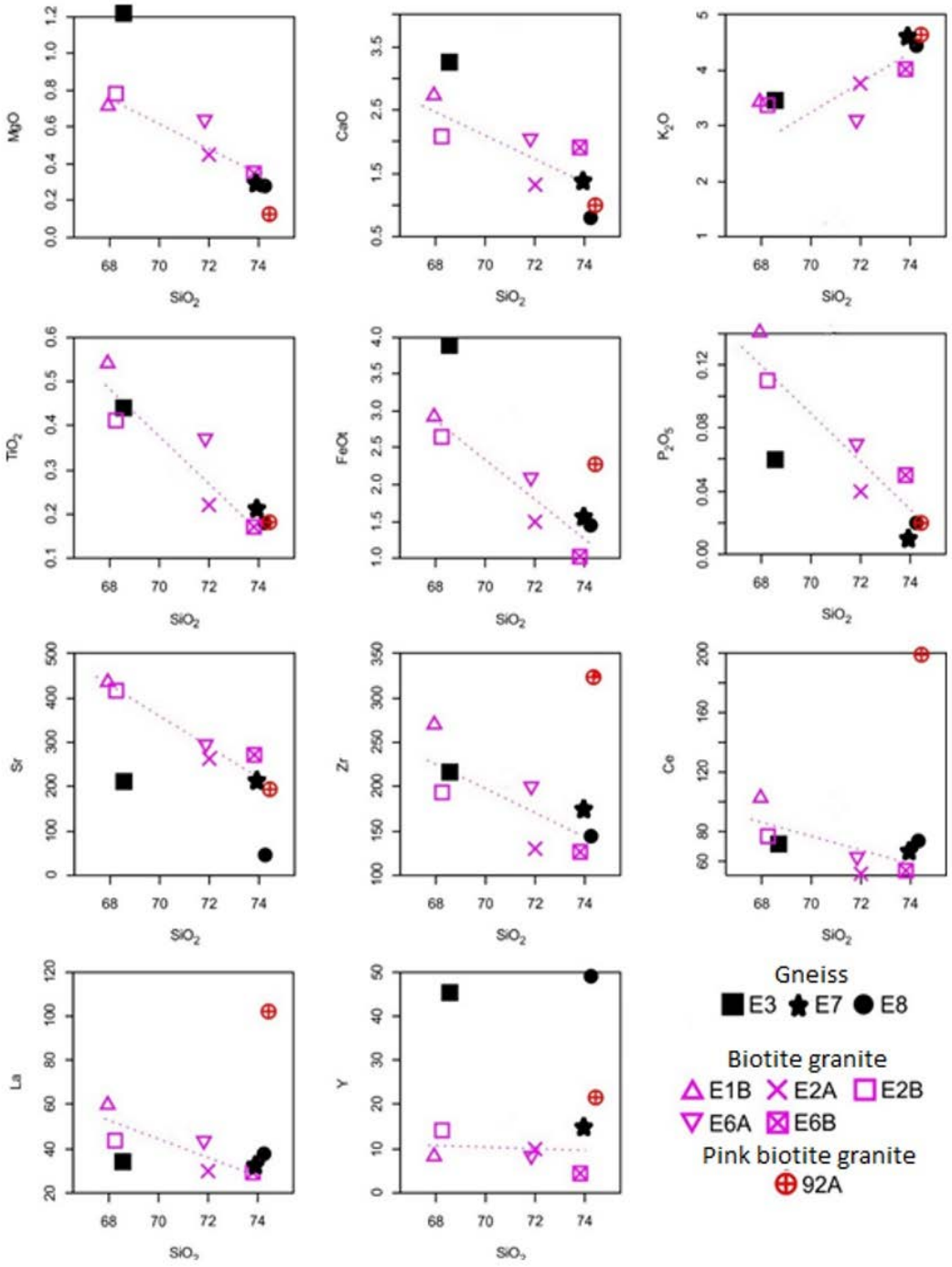

Figure 8 - Harker-type diagrams for major and trace elements versus SiO_2 for the Januária High samples (adapted from Rezende et al., 2018).

Zircon U-Pb Geochronology

Prismatic is the common morphology of the zircons found in gneisses and granites from Januária High.

Laser shots positions in core and rim portions of some zircons can be seen in figure 9. Samples E7 and E8 from gneisses and samples E2A e 92A from granites have been chosen for zircon U-Pb geochronology. U-Pb isotopic data of gneisses and granites from Januária High can be found in Appendix.

The upper and lower intercepts of the U-Pb discordia for gneissic sample E7 reveal ages of 2641 +/- 22 Ma and 1006 +/- 26 Ma respectively (Figure 9A). The upper and lower intercepts of the U-Pb discordia for gneissic sample E8 reveal ages of 2609 +/- 27 Ma and 371.8 +/- 5.6 Ma respectively (Figure 9B). So, gneissic rocks are Neoarchean, differently from granitic ones, which are Paleoproterozoic (Rhyacian). The upper and lower intercepts of the U-Pb discordia for granitic sample E2A show ages of 2186 +/- 10 Ma and 365 +/- 31 Ma respectively. The upper and lower intercepts of the U-Pb discordia for pink granitic sample 92A show ages of 2139.6 +/- 8.4 Ma and 320.1 +/- 8.2 Ma respectively.

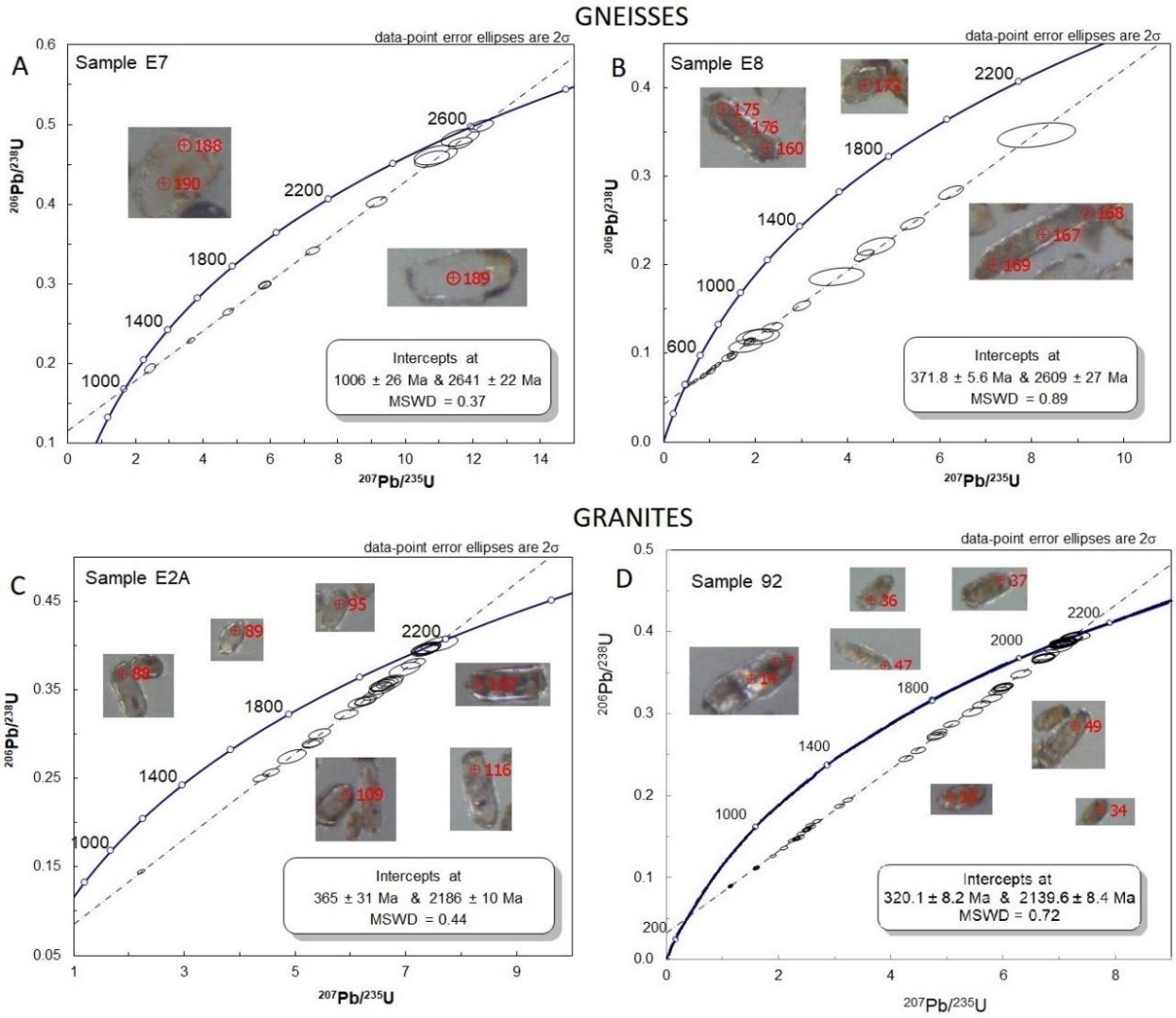

Figure 9 - (A and B) $^{206}Pb/^{238}U$ versus $^{207}Pb/^{235}U$ discordia diagrams for gneisses from Januária High. **(C and D)** $^{206}Pb/^{238}U$ versus $^{207}Pb/^{235}U$ discordia diagrams for granites from Januária High. Some analyzed zircons with labeled laser spots are shown.

DISCUSSION AND CONCLUSIONS

Based on the frequency and range of accessible data preserved in rock record of the continental lithosphere, Cawood et al. (2022) divide the secular evolution of the Earth system into seven phases: (a) "*Proto-Earth*" (ca. 4.57–4.45 Ga); (b) "*Primordial Earth*" (ca. 4.45–3.80 Ga); (c) "*Primitive Earth*" (ca. 3.8–3.2 Ga); (d) "*Juvenile Earth*" (ca. 3.2–2.5 Ga); (e) "*Youthful Earth*" (ca. 2.5–1.8 Ga); (f) "*Middle Earth*" (ca. 1.8–0.8 Ga); and (g) "*Contemporary Earth*" (since ca. 0.8 Ga). Integrating this record with knowledge of secular cooling of the mantle and lithospheric rheology constrains the changes in the tectonic modes that operated through Earth history. Initial accretion and the Moon forming impact during the *Proto-Earth phase* likely resulted in a magma ocean. The solidification of this magma ocean produced the *Primordial Earth* lithosphere, which preserves evidence for intra-lithospheric reworking of a rigid lid, but which also likely experienced partial recycling through mantle overturn and meteorite impacts. Evidence for craton formation and stabilization from ca. 3.8 to 2.5 Ga, during the *Primitive and Juvenile Earth phases*, likely reflects some degree of coupling between the convecting mantle and a lithosphere initially weak enough to favor an internally deformable, squishy-lid behavior, which led to a transition to more rigid, plate like, behavior by the end of the early Earth phases. The *Youthful to Contemporary phases of Earth*, all occurred within a plate tectonic framework with changes between phases linked to lithospheric behavior and the supercontinent cycle (Cawood et al., 2022).

Under the perspective of this evolution of the Earth system, it can be seen that 2.61-2.64 Ga Januária High orthogneisses are inserted in the

context of almost rigid behavior of the lithosphere, by the end of the *Juvenile Earth phase* in the Neoarchean. However, the form of plate tectonic processes that operated during this time remains contentious, as the mantle was still warmer when compared to its modern thermal state (Cawood et al., 2022). These gneisses are High-K calc-alkaline, meta- to peraluminous (Figs. 7C, 7D, 7E) and their protoliths are the representative in the SFC nucleus of the change in the composition of felsic magmatism found within archean cratons from the Na-rich tonalite–trondhjemite–granodiorite (TTG) suite to more potassic magmatic rocks from around 2.8 Ga to 2.6 Ga worldwide, and is a defining characteristic of the *Juvenile phase* (Laurent et al., 2014). By the way, similar High-K gneiss are also found in southern (Romano et al. 2013) and northern (Zincone et al., 2021) SFC.

The compositional character of K-granitoids requires their formation at shallow depths (<35 km) either via partial melting of pre-existing TTG crust, like the 3.3 Ga TTG gneisses of the adjacent DPT and DGC (Silva et al., 2016; Barbosa et al., 2020), or via fractionation crystallization of TTG melts. Low-degree melting of hydrated metabasalts can also produce K-granitoids but such low melt fractions are unlikely to form extensive batholiths unless huge amount of basalts participate in melting (Laurent *et al*., 2014). Thus, the protolith origin of the 2.61-2.64 Ga High-K Januária orthogneisses is suggestive of intracrustal partial melting of local TTG (according to Fig. 7M and with plagioclase retained in the source as revealed by their huge Eu negative anomalies – Fig. 7I) followed by local deformation, metamorphism e migmatization, as occurred with 2.6 to 2.7 Ga gneisses found in adjacent DPT and DGC (Silva *et al*., 2016; Barbosa et al., 2020).

Evidence for widespread dyke emplacement into brittle cratonic crust become globally distributed through the Paleoproterozoic. These dykes, along with the development of rift and passive margin sedimentation along the edges of a number of cratons, provides evidence for subsidence associated with lithospheric extension. This, together with the development of linear late Paleoproterozoic collisional orogenic belts, suggests a pattern of oceans opening and closing associated with a globally linked pattern of focused plate boundaries (Cawood *et al*., 2022). This led to the assembly of the Archean cratons into the first supercontinent Columbia (Nuna) by the late Paleoproterozoic (Zhao et al., 2002; Chaves, 2021). Commencing in the late Archean, but mainly from the Paleoproterozoic to the present day, the presence for globally distributed passive margins along the edges of pre-existing continental fragments, linear belts of accretionary and collisional orogens with associated tectonothermal events, and paleomagnetic data indicative of relative motion of continental fragments argues for a linked system of divergent and convergente plate margins that formed in an active lid, plate tectonic regime (Cawood et al., 2022).

Supported on this clear evidence of the plate tectonic activity in Paleoproterozoic, it can be seen that 2.14-2.19 Ga Januária High biotite granites are inserted in the context of *Youthful Earth phase*. Similar 2.14 Ga granitoids are also found in adjacent DGV and DPT (Cruz et al., 2016; Silva et al., 2016), which together with the Januária High granites, are the record of accretionary orogeny delineated by the edification of a magmatic arc, as suggested by Cruz et al. (2016) for DGV (named as Western Bahia arc) and Rezende et al. (2018) for Januária High intracratonic region. The comparison between this arc tectonic model and other existing models that explain the Siderian-Rhyacian-Orosirian granitogenesis of the Mineiro Belt (CMI) suggests a continuation of the Western Bahia Magmatic Arc and of the collisional orogen that followed, towards the southern SFC (Cruz et al., 2016).

The existence of such an arc in Januária High is supported on lithochemical data, which shows that local 2.14-2.19 Ga biotite granites are calc-alkaline, I-type rocks (Figs. 7C, 7F, 7G and 7H) typical or subduction-related continental magmatic arcs, as also attested by VAG signature in Pearce tectonic diagrams (Figs. 7K and 7L) and by Ta and Nb negative anomalies (Fig. 7J). In addition, their REE patterns are similar to those of the Peruvian coastal batholith of the Andean magmatic arc (Fig. 7I). These High-K biotite granites are probably derived from a High-K mafic source associated with tonalites (Fig. 7M) and their peraluminous signature (Fig. 7D) and normative corundum (Table 3) suggests possible crustal contamination processes during the petrogenesis.

Figure 10 presents a tectonic model for the *Youthful Earth phase* pictured by the paleoproterozoic rocks of the Januária High in the SFC nucleus. Adapted from the evolution of the

Western Bahia Magmatic Arc (Cruz et al., 2016), at 2.15 Ga the same arc in the Januária High region is represented by the intrusion of the Rhyacian biotite granites during the regional subduction-related accretionary orogeny. The metamorphic peak would be attained during the collision between nearby older continental blocks like DJQ, DGC, DGV and DPT at 2.10 Ga.

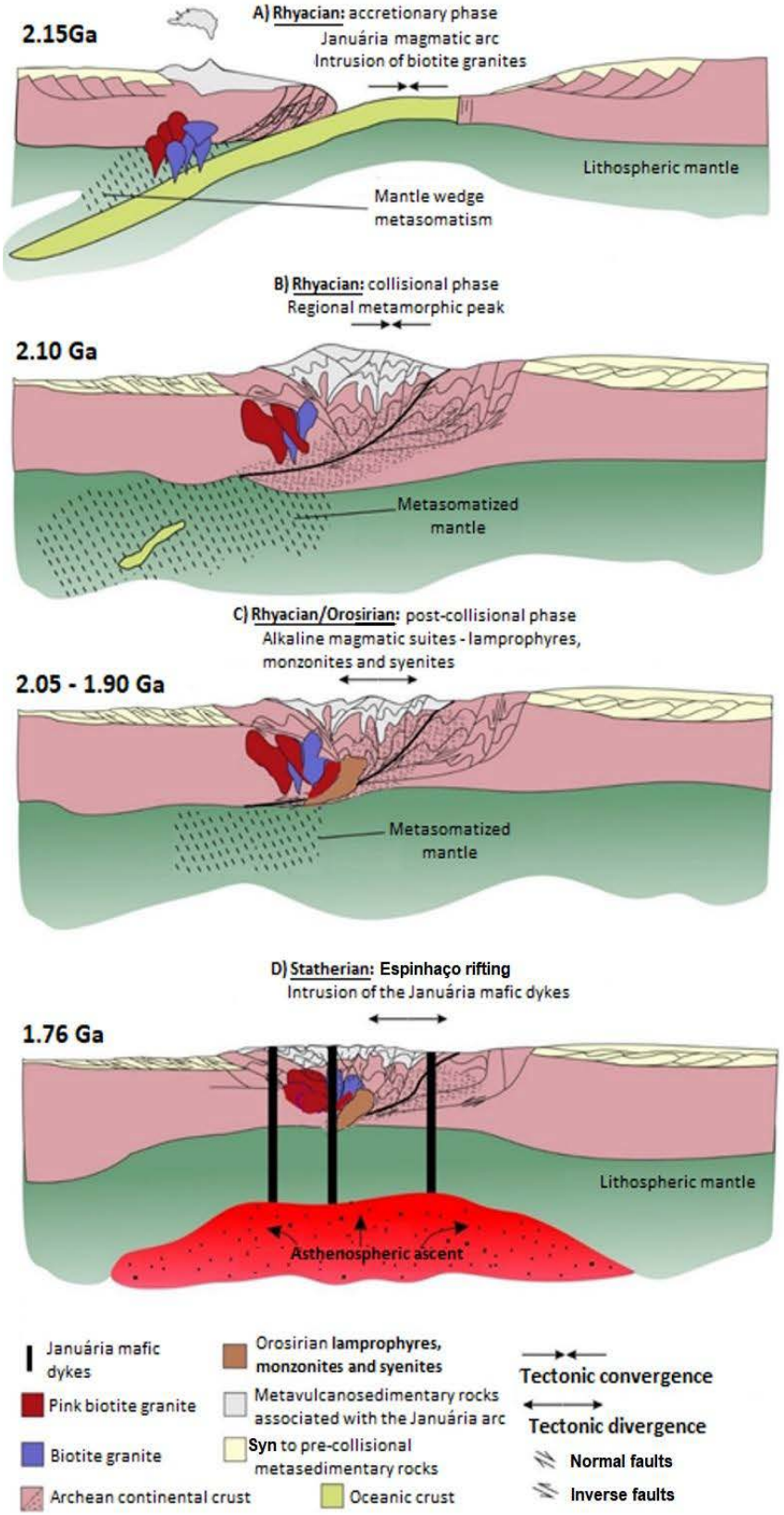

Figura 10 - Schematic model of Paleoproterozoic tectonic evolution for the Januária High. **(A)** Installation of the magmatic arc in the continent-ocean convergence zone during the Rhyacian, with intrusion of the biotite granites. **(B)** Metamorphic peak during the Rhyacian collisional phase. **(C)** Orogenic collapse and injection of lamprophyres into the biotite granites. **(D)** Intrusion of the Januária mafic dykes associated with the opening of the Espinhaço rift. Modified from Cruz et al. (2016) and Rezende et al. (2018).

Following this collisional phase at the beginning of Orosirian, between 2.05 and 1.90 Ga, would have occurred the post-collisional phase marked by the injection of lamprophyric (Fig. 5D), monzonitic and syenitic (like 2.05 Ga Guanambi batolith of DGC - Barbosa et al., 2020 - and 2.05 Ga Paciência suite – Sena et al., 2018) alkaline rocks, which belongs to the 2.05-1.90 Ga Minas-Bahia Alkaline Province of Chaves (2015). Finally, at 1.76 Ga occurred the emplacement of the Januária mafic dykes (Chaves & Rezende, 2019) in gneisses and granites of Januária High, during the initial stages of the Espinhaço rifting (Figs. 3A and 3B).

ACKNOWLEDGEMENTS

We thank CNPq for research productivity grant of the first author, Cristiano Lana for support on geochronology and A. C. Pedrosa Soares for support on field work.

REFERENCES

ALKMIM, F.F. & MARSHARK, S. The Transamazonian orogeny in the Quadrilatero Ferrifero, Minas Gerais, Brazil: Paleoproterozoic Collision and Collapse in the Souhtern Sao Francisco Craton region. **Precambrian Research**, v. 90, n. 1, p. 29–58, 1998. DOI: <https://doi.org/10.1016/S0301-9268(98)00032-1>.

ALKMIM, F.F. & MARTINS-NETO, M.A. A bacia intracratônica do São Francisco: Arcabouço estrutural e cenários evolutivos. In: C.P., PINTO; M.A.; MARTINS NETO, (etds.) **Bacia do São Francisco: Geologia e Recursos Naturais**, Belo Horizonte, SBG/MG, Belo Horizonte, p. 9-30, 2001.

ALKMIM, F.F.; BRITO NEVES, B.B.; CASTRO ALVES, J.A. Arcabouço tectônico do Cráton do São Francisco: uma revisão. In: J.M.L. DOMINGUEZ; A. MISI. **O Cráton do São Francisco**. SBG/SGM/CNPq, Salvador, p. 45-62, 1993.

ALMEIDA, A.M. de & UCHIGASAKI, K. **Mapeamento geológico em área dos municípios de Cônego Marinho e Januária – MG.** Belo Horizonte. 2003. p. 83. Trabalho de Graduação. Universidade Federal de Minas Gerais.

ATHERTON, M.P.; MCCOURT, W.J.; SANDERSON, L.M.; TAYLOR, W.P. The geochemical character of the segmented Peruvian Coastal Batholith and associated volcanics. In: ATHERTON, M.P. & TARNEY, J. **Origin of Granite Batholiths: Geochemical Evidence**, p. 334, 1979.

ÁVILA, C.A.; TEIXEIRA, W.; CORDANI, U.G.; MOURA, C.A.V.; PEREIRA, R.M. Rhyacian (2.23–2.20 Ga) juvenile accretion in the southern São Francisco craton, Brazil: geochemical and isotopic evidence from the Serrinha magmatic suite, Mineiro belt. **Journal of South American Earth Sciences**, v.29(2), p. 464–482, 2010.

BABINSKI, M. & KAUFMANN, A.J. **First direct dating of a Neoproterozoic post-glacial cap carbonate.** In: SOUTH AMERICAN SYMPOSIUM ON ISOTOPE GEOLOGY, v. 4, Salvador, 2003. **Short Papers**…Salvador: Sociedade Brasileira de Geologia, v.1, p. 321-323, 2003.

BABINSKI, M. **Idades isocrônicas Pb/Pb e geoquímica isotópica de Pb das rochas carbonáticas do Grupo Bambuí, na porção sul da Bacia do São Francisco.** São Paulo, p. 133, 1993. Tese (Doutorado). Instituto de Pesquisas Energéticas e Nucleares, Universidade de São Paulo.

BABINSKI, M.; CHEMALE, Jr F.; SCHMUS, W.R.V. The Pb/Pb age of minas Supergroup carbonate rocks, Quadrilátero Ferrífero, Brazil. **Precambrian Research**, v. 72, n. 3, p. 235-245, 1995.

BARBOSA, N.; MENEZES LEAL, A.B.; DEBRUYNE, D.; BASTOS LEAL, L.R.; BARBOSA, N.S.; MARINHO, M.; MERCÊS, L.; BARBOSA, J.S.; KOPROSKI, L.M. Paleoarchean to Paleoproterozoic crustal evolution in the Guanambi-Correntina block (GCB), north São Francisco Craton, Brazil, unraveled by U-Pb Geochronology, Nd-Sr isotopes and geochemical constraints. **Precambrian Research,** v. 340, p. 105614, 2020.

BARBOSA, N.S.; TEIXEIRA, W.; ÁVILA, C.A.; MONTECINOS, P. M.; BONGIOLO, E. M. 2.17-2.10 Ga plutonic episodes in the mineiro belt, São Francisco Craton, Brazil: U-Pb ages, geochemical constraints and tectonics**. Precambrian Research**, v. 270, p. 204-225, 2015.

BEURLEN, H. **Ocorrências de chumbo, zinco e fluorita nas rochas sedimentares do Precambriano Superior no Grupo Bambuí em Minas Gerais (Brasil Central).** Heilderberg, p. 165, 1973. Tese (Doutorado). (tradução do autor). Faculdade de Ciências Naturais, Universidade Karl Ruprecht.

BOYNTON, W.V. Cosmochemistry of the rare earth elements; meteorite studies. In: Rare earth element geochemistry. **Elsevier Science Publishing Co.**, v. 2, p. 63-114, 1984.

CAMPOS, J.C.S. & CARNEIRO, M.A. Neoarchean and Paleoproterozoic granitoids marginal to the Jeceaba-Bom Sucesso lineament (SE border of the southern São Francisco craton): genesis and tectonic evolution. **Journal of South American Earth Sciences,** v. 26, n. 4, p. 463–484, 2008.

CAWOOD, P. A.; CHOWDHURY, P.; MULDER, J.A.; HAWKESWORTH, C. J.; CAPITANIO, F. A.; GUNAWARDANA, P. M.; NEBEL, O. Secular evolution of continents and the Earth system. **Reviews of Geophysics,** v. 60, 2022. DOI: <https://doi.org/10.1029/2022RG000789>.

CHAPPELL, B.W. & WHITE, A.J.R. Two contrasting granite types: 25 years later. **Australian Journal of Earth Sciences**, v. 48, p. 489-499, 2001.

CHAVES, A.O. & CORREIA NEVES, J.M. Radiometric ages, aeromagnetic expression, and general geology of mafic dykes from southeastern Brazil and implications for African-South American correlations. **Journal of South American Earth Sciences**, v. 19, p.3 87-397. 2005.

CHAVES, A.O. & REZENDE, C.R. Fragments of 1.79-1.75 Ga large Igneous Provinces in reconstructing Columbia (Nuna): a Statherian supercontinent-superplume coupling? **Episodes**, v. 42, n. 1, p. 55–67, 2019.

CHAVES, A.O. Columbia (Nuna) supercontinent with external subduction girdle and concentric accretionary, collisional and intracontinental orogens permeated by large igneous provinces and rifts. **Precambrian Research,** v. 352, p. 106017, 2021. DOI: <https://doi.org/10.1016/j.precamres.2020.106017 >.

CHAVES, A.O. Correlações entre suítes magmáticas alcalinas orosirianas pós-colisionais da Bahia e de Minas Gerais: fragmentos de uma província alcalina? **Boletim do Museu Paraense Emílio Goeldi. Ciências Naturais,** v. 10, n. 2, p. 179-197, 2015. DOI:<https://doi.org/10.46357/bcnaturais.v10i2.480 >.

CHAVES, A.O.; PIRES, A.C.C.; BRASIL, M.F.A. New knowledge update on mafic dyke swarms of Minas Gerais (Brazil): fragments of ancient large igneous provinces highlighted by aeromagnetometry**. Brazilian Journal of Geophysics,** v. 39, n. 2, p. 227-235, 2021.

CODEMIG, Companhia de Desenvolvimento Econômico de Minas Gerais. **Mapa Geológico MG.** Mapa Geológico do Estado de Minas Gerais, Escala 1:1.000.000, CD-ROM. 2014.

CORDANI, U.G.; SATO, K.; TEIXEIRA, W.; TASSINARI, C.C.G.; BASEI, M.A.S. Crustal Evolution of the South American Platform. In: CORDANI, U.G.; MILANI, E.J.;

THOMAZ, F.; CAMPOS, D.A.; DIOGENES, A. **Tectonic Evolution of South America**, 31st INTERNATIONAL GEOLOGICAL CONGRESS, Rio de Janeiro, p. 19-40, 2000.

COSTA, M.T. & BRANCO, J.J.R. **Introdução.** In: BRANCO, J.J.R. Roteiro para a excursão a Belo Horizonte – Brasília. In: CONGRESSO BRASILEIRO DE GEOLOGIA, v. 14, Belo Horizonte, 1961. **Anais**...Belo Horizonte: Sociedade Brasileira de Geologia, 1961, v. 15, p. 1-119,

COSTA, P.C.G. **Geologia das Folhas de Januária, Mata do Jaíba, Japoré e Manga, Minas Gerais. Memória Técnica.** CETEC. Belo Horizonte, 1978.

CRUZ, S.C.P.; BARBOSA, J.S.F.; PINTO, M.S.; PEUCAT, J.J.; PAQUETTE, J.L.; SOUZA, J.S.; MARTINS, V.S.; CHEMALE, Jr. F.; CARNEIRO, M.A. The Siderian-Orosirian magmatism in the Archean Gavião Paleoplate, Brazil. **Journal of South American Earth Sciences,** v. 69, p. 43-79, 2016.

DIAS-BRITO, D.; PESSAGNO, E.A.J.; CASTRO, J.C. **Novas considerações cronoestratigráficas sobre o silexito a radiolários da Bacia Sanfranciscana, Brasil, e a ocorrência de foraminíferos planctônicos nestes depósitos.** In: 5° SIMPÓSIO SOBRE EL CRETÁCICO DE AMÉRICA DEL SUR, Serra Negra. **Boletim**... Rio Claro: IGCE - UNESP, v. 1. p. 567-575, 1999.

FROST, B. R.; BARNES, C. G.; COLLINS, W. J.; ARCULUS, R. J.; ELLIS, D. J.; FROST, C. D. A geochemical classification for granitic rocks. **Journal of Petrology,** v. 42, p. 2033–2048, 2001.

GEOBANK. Formação Lagoa do Jacaré: idades. **CPRM - Companhia de Pesquisa de Recursos Minerais - Serviço Geológico do Brasil,** 2015a. Disp. em: http://geobank.cprm.gov.br/pls/publico/litoestratigrafia.Litoestratigrafia_Datacoes.Cadastro?p_COD_UNIDADE_ESTRAT=702&p_bb_idade_sigla=NP3&p_comando=cadastro&p_sigla=NP3lj&p_webmap=N. Acesso em: 17agos2015.

GEOBANK. Formação Serra de Santa Helena: idades. **CPRM - Companhia de Pesquisa de Recursos Minerais - Serviço Geológico do Brasil,** 2015b. Disp. em: http://geobank.cprm.gov.br/pls/publico/litoestratigrafia.Litoestratigrafia_Datacoes.Cadastro?p_COD_UNIDADE_ESTRAT=2095&p_bb_idade_sigla=NP3&p_comando=cadastro&p_sigla=NP3sh&p_webmap=N. Acesso: 17agos2015.

GEOBANK. Grupo Urucuia: idades. **CPRM - Companhia de Pesquisa de Recursos Minerais - Serviço Geológico do Brasil,** 2015c. Disp. em: http://geobank.cprm.gov.br/pls/publico/litoestratigrafia.Litoestratigrafia_Datacoes.Cadastro?p_COD_UNIDADE_ESTRAT=406&p_bb_idade_sigla=K2&p_comando=cadastro&p_sigla=K2u&p_webmap=N. Acesso: 17agos2015.

GERDES, A. & ZEH, A. Combined U–Pb and Hf isotope LA-(MC-)ICP-MS analyses of detrital zircons: Comparison with SHRIMP and new constraints for the provenance and age of an Armorican metasediment in Central Germany. **Earth and Planetary Science Letters,** v. 249, n. 1, p. 47-61, 2006. DOI: <10.1016/j.epsl.2006.06.039>.

HORSTWOOD, M.S.A.; KOŠLER, J.; GEHRELS, G.; JACKSON, S.E.; MCLEAN, N.M.; PATON, C.; PEARSON, N.J.; SIRCOMBE, K.; SYLVESTER, P.; VERMEESH, P.; BOWRING, J.F. Community-Derived Standards for LA-ICP-MS U-(Th-) Pb Geochronology–Uncertainty Propagation, Age Interpretation and Data Reporting. **Geostandards and Geoanalytical Research,** v. 40, p. 311-332, 2016.

IGLESIAS, M. **Estratigrafia e tectônica do Grupo Bambuí no norte do Estado de Minas Gerais.** Belo Horizonte, p. 121, 2007. Dissertação (Mestrado), Universidade Federal de Minas Gerais.

LAURENT, O.; MARTIN, H.; MOYEN, J.F.; DOUCELANCE, R. The diversity and evolution of late-Archean granitoids: Evidence for the onset of "modern-style" plate tectonics between 3.0 and 2.5 Ga. **Lithos**, v. 205, p. 208-235, 2014.

LE BAS, M.J.; LE MAITRE, R.W.; STRECKEISEN, A.; ZANETTIN, B. A chemical classification of volcanic rocks based on the total alkali–silica diagram. **Journal of Petrology,** v. 27, p. 745–750, 1986.

LUDWING, K. R. "Users Manual for Isoplot/Ex rev. 2.49". A Geochronological Toolkit for Microsoft Excel," **Berkeley Geochronology Center Special Publication,** v. 1, p. 1-55, 2001.

MACHADO, N.; NOCE, C.M.; OLIVEIRA, O.A.B.; LADEIRA, E.A. Evolução geológica do Quadrilátero Ferrífero no Arqueano e Proterozoico inferior, com base na geocronologia U-Pb. In: V Simpósio de Geologia de Minas Gerais. SBG. **Anais**, v. 10, p. 1-4, 1989.

NOBRE-LOPES, J. **Diagenesis of the dolomites hosting Zn/Ag mineral deposits in the Bambui Group at Januaria Region-MG**. PhD Thesis, University of Campinas, Campinas, São Paulo, Brazil, 183 p. 2002.

NOCE, C.M.; PEDROSA-SOARES, A.C.; SILVIA, L.C.; ARMSTRONG, R.; PIUZANA, D. Evolution of polycyclic basement complexes in the Araçuaí Orogen based on U–Pb SHRIMP data: implications for Brazil–Africa links in Paleoproterozoic time. **Precambrian Research,** v. 159, p. 60–78, 2007.

NOCE, C.M.; TEIXEIRA, W.; QUÉNEUR, J.J.G.; MARTINS, V.T.S.; BOLZACHINI; E. Isotopic signatures of Paleoproterozoic granitoids from southern São Francisco Craton, NE Brazil, and implications for the evolution of the Transamazonian Orogeny. **Journal of South American Earth Sciences**, v. 13, p. 225-239, 200.

PAULSEN, S.; BOSUM, W.; HAGEN, D.; LACERDA, G.M.; LIMA, J.E.S.; RIBEIRO, C.I.; GODOY, A.; SOUZA, A.A.; BICALHO, F.D.; FERRARI, P.G.; HEINECK, C.; STEINER, H.P.; PAULINO, J.; RITCHER, P.; LANHER, L.; MOLLAT, H.; RESCH, M.; OSWALD, J.; JOCHMANN, D. **Relatório de reconhecimento geológico geoquímico Pratinha-Argenita-Tapira-Serra da Canastra, Minas Gerais.** CPRM/DNPM/ Serviço Geológico da República da Alemanha (Convênio Geofísica Brasil – Alemanha), p. 57, 1974.

PEARCE, J.A. Role of the sub-continental lithosphere in magma genesis at active continental margins. In: HAWKESWORTH, C.J. & NORRY, M.J. **Continental basalts and mantle xenoliths**. Shiva Publishers, Cheshire, Uk., p. 230-256, 1983.

PEARCE, J.A. Sources and settings of granitic rocks. **Episodes**, v. 19, n. 4, p. 120-125, 1996.

PEARCE, J.A.; HARRIS, N.B.W.; TINDLE, A.G. Trace element discrimination diagrams for the tectonic interpretation of granitic rocks. **Journal of Petrology,** v. 25, p. 956-983, 1984.

PECCERILLO, A. & TAYLOR, S.R. Geochemistry of Eocene calc-alkaline volcanic rocks from the Kastamonu area, Northern Turkey. **Contributions to Mineralogy and Petrology,** v. 58, p. 63–81, 1976.

PEDROSA-SOARES, A.C. & ALKMIM, F.F. How many rifting events preceded the development of the Araçuaí-west Congo Orogen? **Geonomos.** Edição Especial - 30 Anos do CPMTC, v. 19(2), 2011.

PEDROSA-SOARES, A.C.; NOCE, C.M.; WIEDMANN, C.M.; PINTO, C.P. The Araçuaí-West Congo orogen in Brazil: an overview of a confined orogen formed during Gondwanland assembly. **Precambrian Research.,** v. 110, p. 307-323, 2001.

PFLUG, R. & RENGER, F. **Estratigrafia e evolução geológica da margem sudeste do Cráton Sanfranciscano**. In: CONGRESSO BRASILEIRO DE GEOLOGIA, XXVII, Aracaju, 1973. **Anais**...Aracaju: Sociedade Brasileira de Geologia, 1973, p. v 25-19.

RADAMBRASIL. 1982. DNPM. **Folha SD.23, Brasília**. Rio de Janeiro, 660 p.

REZENDE, C.R.; CHAVES, A.O.; OLIVEIRA, V.P. Evidências diretas e indiretas de arco magmático paleoproterozoico na região do Alto de Januária – Norte de Minas Gerais. **Geonomos,** v. 26, n. 2, p. 1-22, 2018.

ROMANO, R.; LANA, C.; ALKMIM, F.F.; STEVENS, G.; ARMSTRONG, R. Stabilization of the southern portion of the São Francisco Craton, SE Brazil, through a long-lived period of potassic magmatism. **Precambrian Research**, v. 224, p. 143-159, 2013.

SAWYER, E. W. Atlas of Migmatites. Special Publications of The **Canadian Mineralogist**, v. 9, p. 386, 2008.

SEIXAS, L.A.R.; DAVID, J.; STEVENSON, R. Geochemistry, Nd isotopes and U e Pb geochronology of a 2350 ma TTG suite, Minas Gerais Brazil: implications for the crustal evolution of the southern São Francisco craton. **Precambrian Research,** v. 196, p. 61-80, 2012.

SENA, V.H.; OLIVEIRA, A.L.R.; CHAVES, A.O. Petrologia das suítes paleoproterozoicas Paciência e Catolé da porção setentrional do domínio Porteirinha (Minas Gerais). **Geonomos**, v. 26, n. 1, p. 43-50, 2018. DOI: <https://doi.org/10.18285/geonomos.v26i1.1238>.

SILVA, L.C.; ARMSTRONG, R.W.; NOCE, C.M.; CARNEIRO, M.A.; PIMENTEL, M.M.; PEDROSA-SOARES, A.C.; LEITE, C.A.; VIEIRA, V.S; SILVA, M.A.; PAES, J.C.; CARDOSO FILHO, J.M. Reavaliação da evolução geológica em terrenos Pré-cambrianos brasileiros com base em novos dados U–Pb SHRIMP, Parte II: Orógeno Araçuaí, Cinturão Mineiro e Cráton São Francisco Meridional. **Revista Brasileira de Geociências**, v. 32, p. 101–137, 2002.

SILVA, L.C.; PEDROSA-SOARES, A.C.; ARMSTRONG, R.; PINTO, C.P.; MAGALHÃES, J.T.R.; PINHEIRO, M.A.P.; SANTOS, G.G. Disclosing the Paleoarchean to Ediacaran history of the São Francisco craton basement: The Porteirinha domain (northern Araçuaí orogen, Brazil). **Journal of South American Earth Sciences**, v .68, p. 50-67, 2016.

SILVA, L.C.; PEDROSA-SOARES, A.C.; DUSSIN, I. A.; ARMSTRONG, R.; NOCE, C. M. O Complexo Belo Horizonte de Carlos Maurício Noce revisitado. In: CONGRESSO BRASILEIRO DE GEOLOGIA, 46, 2012, Santos. **Anais**...Santos: Sociedade Brasileira de Geologia, 2012, (CD-ROM).

STACEY, J.S. & KRAMERS, J.D. Approximation of Terrestrial Lead Isotope Evolution by a Two-Stage Model. **Earth and Planetary Science Letters,** v. 26, p. 207-221, 1975. DOI: <https://doi.org/10.1016/0012-821X(75)90088-6 >.

STRECKEISEN, A. Classification and nomenclature of plutonic rocks. **Geologische Rundschau,** v. 63, p. 773–786, 1974.

TEIXEIRA, W.; ÁVILA, C.A.; DUSSIN, I. A.; CORRÊA-NETO, A.; BONGIOLO, E.M.; SANTOS, J.O.; BARBOSA, N.S. A juvenile accretion episode (2.35-2.32 Ga) in the mineiro belt and its role to the Minas accretionary orogeny: zircon U-Pb-Hf and geochemical evidences. **Precambrian Research**, v. 256, p. 148-169, 2015.

TEIXEIRA, W.; SABATÉ, P.; BARBOSA, J.; NOCE, C.M.; CARNEIRO, M.A. Archean and tectonic evolution of the São Francisco Craton. In: CORDANI, U.G.; MILANI, E.J.; THOMAS FILHO, A.; CAMPOS, D.A. Tectonic Evolution of South America. In: 31st INTERNATIONAL GEOLOGICAL CONGRESS, Rio de Janeiro, 2000. **Anais**...Rio de Janeiro: Sociedade Brasileira de Geologia, 2000, v. 101-137.

UHLEIN, G. J.; SALGADO, S.S.; UHLEIN, A.; CAXITO, F.A.; MENDES, T.A.A. 2015. **Geologia e Recursos Minerais Folha Catolé (SE.23-Z-C-I)** Escala: 1:100.000. Projeto Fronteiras de Minas/CODEMIG.

WHALEN, J.B.; CURRIE, K.L.; CHAPPELL, B.W. A-type granites: geochemical characteristics, discrimination and petrogenesis. **Contributions to Mineralogy and Petrology**. v. 95, p. 407- 419, 1987.

WHITNEY, D.L. & EVANS, B.W. Abbreviations for names of rock-forming minerals. **American Mineralogist**, v. 95, p. 185-187, 2010.

WINTER, J.D. **An introduction to igneous and metamorphic petrology**. Upper Saddle River, NJ: Prentice Hall, p. 697, 2001.

ZHAO, G.; CAWOOD. P. A.; WILDE, S. A.; SUN, M. Review of global 2.1–1.8 Ga orogens: Implications for a pre-Rodinia supercontinent. **Earth-Science Reviews**, v. 59, n. 1–4, p. 125–162, 2002. DOI: <https://doi.org/10.1016/s0012-8252(02)00073-9 >.

ZINCONE, S.A.; OLIVEIRA, E.P.; RIBEIRO, B.P.; MARINHO, M.M. High-K granites between the Archean Gaviao and Jequie blocks, Sao Francisco Craton, Brazil: Implications for cratonization and amalgamation of the Rhyacian Atlantica continent. **Journal of South American Earth Sciences**, v. 105, p. 102920, 2021.

Submetido em 14 de março de 2023
Aceito para publicação 19 de julho de 2023